MULTIPLICITIES AND RAPIDITY DISTRIBUTIONS ASSOCIATED WITH A LARGE $p_\perp$ TRIGGER

By A. Schiller

Sektion Physik, Karl-Marx-Universität Leipzig*

(Received December 30, 1977)

We assume that the background formed by the spectator constituents in a hard scattering process behaves like a normal low $p_\perp$ event at reduced energy and shifted rapidity corresponding to overall energy-momentum conservation. The model rather well describes the data on multiplicities for trigger $p_\perp > 1.5$ GeV/c. We predict the behaviour of associated multiplicities for trigger exceeding 4 GeV/c. The associated background rapidity distribution is considerably affected at large cms trigger rapidity and with rising trigger transverse momentum.

1. Introduction

In the last years it became apparent that hadron production at large $p_\perp$ is a tool to learn about the interaction mechanism of basic constituents of hadrons [1, 2]. Further properties of the hard collision dynamics can be understood by a study of the detailed structure of events containing large $p_\perp$ particles. We address ourselves here to this problem. So far there is no unique view whether the low $p_\perp$ component resembles the final states obtained with minimum bias trigger [1, 2, 3].

In events with a large $p_\perp$ trigger, a large $p_\perp$ as well as a low $p_\perp$ component are present. In the quark-parton model, the large $p_\perp$ component arises from the hard scattering and fragmentation of partons; the fragments of the partons emerge as hadronic jets. The low $p_\perp$ component is formed by the spectator constituents.

We assume that the low $p_\perp$ system behaves as seen in a usual low $p_\perp$ event. However, due to the presence of the large $p_\perp$ particles, the low $p_\perp$ component has reduced energy and shifted rapidity. Our approach differs from the four jet picture proposed e.g. by Della Negra et al. [3] and Feynman, Field and Fox [5]; in their picture, both the large $p_\perp$ and the low $p_\perp$ component form two jets which fragment in a similar way. We study in particular the average multiplicity and the rapidity distribution associated with a large $p_\perp$

* Address: Sektion Physik, Karl-Marx-Universität, 701 Leipzig, Karl-Marx-Platz, DDR.

trigger. In a more simplified way associated multiplicities at not too large $p_\perp$ were already studied by Abad, Cruz and Alonso [6].

We use in the calculations a hard collision model with elastic quark-quark scattering. As the studies of single particle rapidity distributions and correlations have shown [7–9] such a model with a phenomenological form of the hard scattering cross section $d\sigma/d\hat{t} \sim 1/\hat{s}\hat{t}^3$ describes the meson production at large $p_\perp$ rather well. We use hadron fragmentation functions as in Ref. [8] and quark fragmentation function from a chain decay model of Kripfganz [10].

In Section 2 we describe our model with only kinematical correlations between the large $p_\perp$ and low $p_\perp$ components. In Section 3 the results are discussed and compared with data.

2. *Description of the model*

In the hard scattering process the parton (quark) i from hadron A and parton j from hadron B produce two jets k and l (Fig. 1). We neglect the transverse momenta of partons and their masses. The system of the two jets — the di-jet — is completely described by momentum P_{JJ}, energy E_{JJ} and the transverse momentum $P_\perp$ of one jet

$$P_{JJ} = (x_1 - x_2)\frac{\sqrt{s}}{2}, \qquad E_{JJ} = (x_1 + x_2)\frac{\sqrt{s}}{2}. \tag{2.1}$$

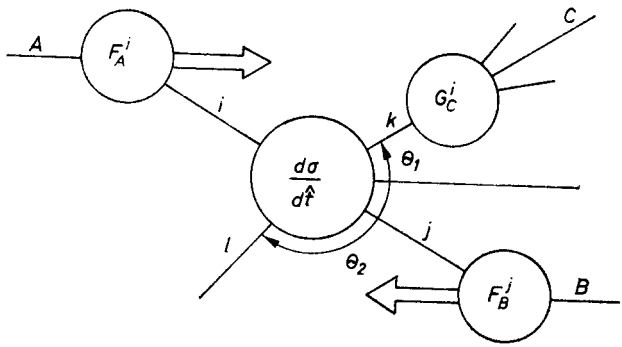

Fig. 1. The hard collision model

The $x_{1,2}$ give the fraction of the hadron momentum carried by the parton i, j. The di-jet cross section may be written as [11]

$$d\sigma \sim \sum_{i,j} F_A^i(x_1)\frac{dx_1}{x_1} F_B^j(x_2)\frac{dx_2}{x_2}\frac{d\sigma^{ij}}{d\hat{t}}\, d\hat{t}. \tag{2.2}$$

Here $d\sigma^{ij}/d\hat{t}$ is the hard scattering cross section; $F(x)$ are the hadron fragmentation functions.

Instead of P_{JJ} and E_{JJ} we introduce the rapidity Y and the invariant mass M of the di-jet system

$$Y = \tfrac{1}{2} \ln \frac{x_1}{x_2}, \qquad M^2 = \hat{s} = x_1 x_2 s. \tag{2.3}$$

Then we obtain for the di-jet production cross section

$$\frac{d\sigma}{dY dM P_\perp dP_\perp} = \sum_{i,j} \frac{4}{\sqrt{M^2 - 4P_\perp^2}} F_A^i\left(\frac{M}{\sqrt{s}} e^{Y}\right) F_B^j\left(\frac{M}{\sqrt{s}} e^{-Y}\right)$$

$$\left\{\frac{d\sigma^{ij}}{d\hat{t}}(M, \hat{t}_1) + \frac{d\sigma^{ij}}{d\hat{u}}(M, \hat{t}_1)\right\} \tag{2.4}$$

with

$$\hat{t}_1 = -\tfrac{1}{2}(M^2 - M\sqrt{M^2 - 4P_\perp^2}). \tag{2.5}$$

After fragmentation into particles we obtain the invariant single particle distribution for production of a large $p_\perp$ particle C from Eq. (2.4)

$$E_C \frac{d^3\sigma}{d^3 p_C} = \frac{1}{2\pi p_{\perp C}} \sum_k \int dY dM \frac{dP_\perp}{P_\perp} I_C^k\left(Y, M, P_\perp, \frac{p_{\perp C}}{P_\perp}\right) \delta(y_C - f(M, Y, P_\perp)) \tag{2.6}$$

with

$$I_C^k\left(Y, M, P_\perp, \frac{p_{\perp C}}{P_\perp}\right) = \frac{d\sigma}{dY dM P_\perp dP_\perp} G_C^k\left(\frac{p_{\perp C}}{P_\perp}\right). \tag{2.7}$$

Here y_C is the rapidity of particle C and $p_{\perp C}$ its transverse momentum; $G_C^k(z)$ is the quark fragmentation function into the observed particle C. The large $p_\perp$ particle C is assumed to arise typically from one of the jets.

The particle rapidity y_C is approximately equal to the single jet rapidity Y_1 if $m_C \ll p_{\perp C}$ and $M_{\text{single jet}} \ll P_\perp$ [12]

$$y_C = Y_1 = -\ln \operatorname{tg} \frac{\theta_1}{2}. \tag{2.8a}$$

For the second jet we find the rapidity

$$Y_2 = -\ln \operatorname{tg} \frac{\theta_2}{2}; \tag{2.8b}$$

θ_1 and θ_2 are the jet production angles in the hadron-hadron cms (Fig. 1). Considering the relations [11]

$$x_1 = \frac{P_\perp}{\sqrt{s}}(e^{Y_1} + e^{Y_2}), \qquad x_2 = \frac{P_\perp}{\sqrt{s}}(e^{-Y_1} + e^{-Y_2}), \tag{2.9}$$

we obtain from the definitions of Y and M (Eq. 2.3)) that

$$Y = \tfrac{1}{2}(Y_1 + Y_2), \quad M^2 = 2P_\perp^2(1+\cosh(Y_1 - Y_2)). \tag{2.10}$$

Using the relations (2.5), (2.7), (2.10) and (2.11) we find

$$y_C = Y - \tfrac{1}{2}\ln\frac{-\hat{t}_1 - P_\perp^2}{P_\perp^2}.$$

Now we can integrate in Eq. (2.8) over Y using the δ-function

$$E_C\frac{d^3\sigma}{d^3p_C} = \frac{1}{2\pi p_{\perp C}}\sum_k \int dM\,\frac{dP_\perp}{P_\perp}\,I_C^k\left(\bar{Y}, M, P_\perp, \frac{p_{\perp C}}{P_\perp}\right) \tag{2.11}$$

with

$$\bar{Y} = y_C + \tfrac{1}{2}\ln\frac{-\hat{t}_1 - P_\perp^2}{P_\perp^2}. \tag{2.12}$$

Particles associated to C can arise from both jets and the low $p_\perp$ background.

Since particle production in low $p_\perp$ events can be reasonably well described by several models (e.g. multiperipheral or uncorrelated cluster models) we use phenomenological fits to data on single particle distributions and multiplicities. If the di-jet system is fixed at Y and M we obtain for the low $p_\perp$ background rapidity and mass

$$Y_{BG} = \tfrac{1}{2}\ln\frac{\sqrt{s} - Me^{-Y}}{\sqrt{s} - Me^{Y}}, \quad M_{BG}^2 = s - 2M\sqrt{s}\cosh Y + M^2. \tag{2.13}$$

The $P_\perp$ of one jet is balanced by the transverse momentum of the other; we do not assume a correlation for the transverse momenta between the large and low $p_\perp$ components. In the cms of the background we parametrize the single particle distribution for the production of particle D with rapidity y_D and low transverse momentum $p_{\perp D}$ in the simple form

$$\Phi(y_D^*, p_{\perp D}, s) = \frac{\langle n(s)\rangle}{\sqrt{2\pi L(s)}}\,e^{-\frac{y_D^{*2}}{2\pi L(s)}}\,\frac{A^2}{2\pi}\,e^{-Ap_{\perp D}}, \quad A \approx 6(\mathrm{GeV}/c)^{-1}. \tag{2.14}$$

The energy dependence of multiplicity $\langle n(s)\rangle$ and rapidity width $L(s)$ is determined from data.

Taking into account overall energy momentum conservation we obtain for the distribution of the background particle D associated to the large $p_\perp$ trigger C the expression (see also Eq. (2.13))

$$\frac{1}{2\pi}\frac{dN}{dy_D p_{\perp D} dp_{\perp D}}\bigg|_{\substack{p_{\perp C}\\ y_C}}$$

$$= \frac{1}{E_C\dfrac{d^3\sigma}{d^3p_C}}\sum_k \int dM\,\frac{dP_\perp}{P_\perp}\,I_C^k\left(\bar{Y}, M, P_\perp, \frac{p_{\perp C}}{P_\perp}\right)\Phi(\bar{Y}_D, p_{\perp D}, \bar{s}) \tag{2.15}$$

with

$$\bar{Y}_D = y_D - \tfrac{1}{2} \ln \frac{\sqrt{\bar{s}} - Me^{-\bar{Y}}}{\sqrt{\bar{s}} - Me^{\bar{Y}}}, \qquad \bar{s} = s - 2M\sqrt{s}\cosh \bar{Y} + M^2. \tag{2.16}$$

$\bar{Y}$ is defined in Eq. (2.12), $E_C d^3\sigma/d^3p_C$ is the invariant single particle distribution of trigger C (see Eq. (2.11)). If we are interested in the whole distribution associated to C we have to add the associated large $p_\perp$ component arising from the jets emerging on the trigger side and on the opposite side. A possibility to obtain this component is described in detail in papers of Ilgenfritz et al., Ranft and Ranft [8, 13]; we shall not repeat the formulae here.

We assume the background multiplicity to be the same as in normal low $p_\perp$ events at the correspondingly reduced energy. We find

$$\langle n \rangle^{\mathrm{BG}}\Big|_{\substack{p_{\perp C} \\ y_C}} = \frac{1}{E_C \dfrac{d^3\sigma}{d^3p_C}} \int dM \frac{dP_\perp}{P_\perp} I_C^k\left(\bar{Y}, M, P_\perp \frac{p_{\perp C}}{P_\perp}\right) \langle n(\bar{s}) \rangle \tag{2.17}$$

with $\bar{Y}$ and $\bar{s}$ given in Eqs. (2.12) and (2.16). The associated multiplicity from the two jets is calculated as indicated in Ref. [13]. Thus we obtain for the total multiplicity depending on $p_{\perp C}$ and y_C

$$\langle n \rangle\Big|_{\substack{p_{\perp C} \\ y_C}} = \langle n \rangle^{\mathrm{BG}}\Big|_{\substack{p_{\perp C} \\ y_C}} + \underbrace{\langle n \rangle\Big|_{\substack{p_{\perp C} \\ y_C}}}_{\text{same side jet}} + \underbrace{\langle n \rangle\Big|_{\substack{p_{\perp C} \\ y_C}}}_{\text{opposite side jet}} . \tag{2.18}$$

We restrict ourselves to the production of large $p_\perp$ meson triggers in pp collisions. Therefore we do not expect significant differences for the associated multiplicity by changing the charge of the meson trigger.

3. Discussion and comparison with experiment

In this Section we compare our model with data and predict the multiplicity behaviour for larger trigger transverse momenta. At relatively small $p_{\perp C}$ other mechanisms than hard scattering may be important for the production of the trigger particle; therefore we analyse multiplicities associated to triggers with $p_{\perp C} > 1.5$ GeV/c. In this case the trigger is expected to result from one of the large $p_\perp$ jets. We use data from the Pisa–Stony Brook collaboration [14] on the charged particle multiplicities associated with large transverse momentum photons for different cms energies.

In our calculations the cross section for the elastic quark-quark scattering $d\sigma/d\hat{t}$ is parametrized as in Refs [7, 8]; the leading term of this parametrization corresponds to $d\sigma/d\hat{t} \sim 1/\hat{s}\hat{t}^3$.

In Fig. 2 our predictions are shown for associated multiplicities of the background and large $p_\perp$ component, resp., versus trigger $p_{\perp C}$ for different cms energies at $y_C = 0$ in pp collisions. In (2.17) we have used a fit for the multiplicities $\langle n(\bar{s}) \rangle$ from Thome et al.

[15]. The background multiplicity decreases almost linearly, near the kinematical boundary it decreases somewhat stronger. With rising $\sqrt{s}$ the slope is less pronounced. In the large $p_\perp$ component there is essentially no $\sqrt{s}$ dependence except near the kinematical boundary. The multiplicity rises logarithmically with increasing $p_{\perp C}$ [16].

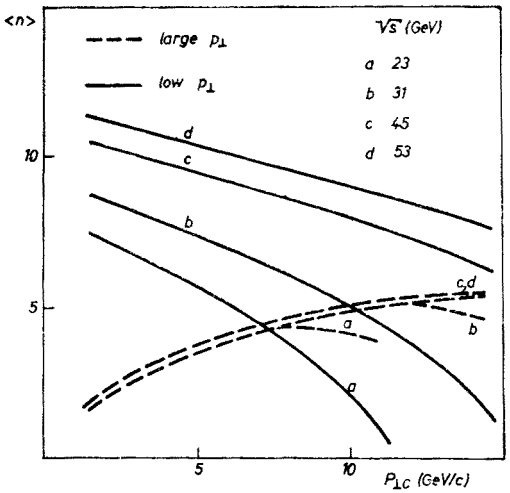

Fig. 2. The multiplicities of the low $p_\perp$ background and the large $p_\perp$ components associated with a large $p_\perp$ trigger vs trigger transverse momentum $p_{\perp C}$. The trigger rapidity is $y_C = 0$, different cms energies are plotted

The presence of a large $p_\perp$ trigger leads to trigger bias effects. Even for rather small trigger transverse momentum, the low $p_\perp$ component does still not resemble normal low $p_\perp$ events since the presence of a trigger (usually with small rapidity) excludes diffractive and quasielastic events. Thus the absence of 2 prong events at the charged multiplicity in the ISR range leads to a rise of the multiplicity of about 20%.

In Fig. 3 we plot the associated charged multiplicity as function of the trigger $p_{\perp C}$ at $y_C = 0$ for different $\sqrt{s}$. The data points are taken from Ref. [14]. The trigger bias effect mentioned above is taken into account. For rising trigger $p_{\perp C}$ we predict a flattening of the multiplicity followed by a decrease towards the kinematical boundary.

In Fig. 4 the associated same and opposite side multiplicities versus $p_{\perp C}$ at $\sqrt{s} = 45$ and 53 GeV are compared to data from Ref. [14]. For $p_{\perp C} > 4$ GeV/c we expect the same side multiplicity to decrease smoothly with $p_{\perp C}$ whereas the opposite side multiplicity does still increase, although its slope decreases.

The model describes the qualitative behaviour of the data on multiplicities. To explain the right magnitude of the same and opposite side multiplicities the effect of bias due to parton transverse momenta has to be taken into account [17]. Therefore the low $p_\perp$ multiplicity on the opposite side is somewhat enhanced. Simultaneously the multiplicity of the opposite side jet is slightly decreased. But this decrease is smaller than the increase of low $p_\perp$ multiplicity.

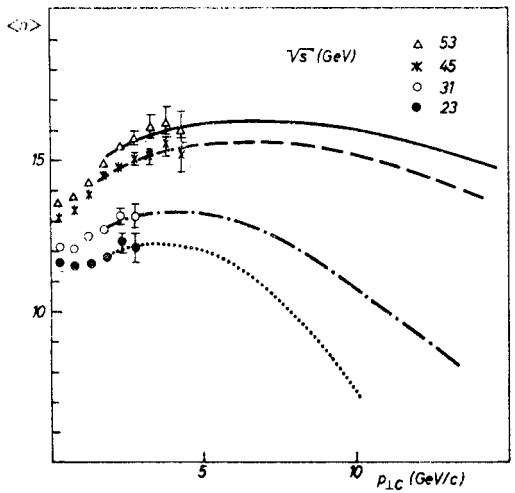

Fig. 3. Associated charged multiplicities as function of $p_{\perp C}$ at $y_C = 0$ for different cms energies. Comparison of the model with data from Ref. [14]

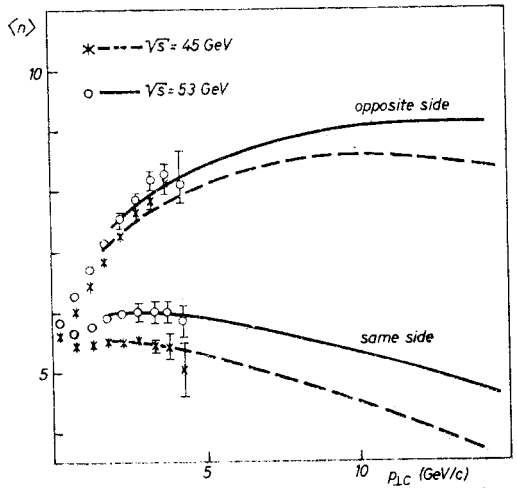

Fig. 4. Associated charged same and opposite side multiplicities as function of $p_{\perp C}$ at $y_C = 0$ for $\sqrt{s} = 45$ GeV and 53 GeV. Data points are taken from Ref. [14]

Next we investigate the rapidity distribution of the low $p_\perp$ component. With the presence of the large $p_\perp$ trigger not only the average multiplicity but also the rapidity distribution has to change. In Fig. 5 we compare, according to (2.15), the calculated low $p_\perp$ rapidity distribution for negative particles associated to a large $p_\perp$ trigger particle C at different $p_{\perp C}$ and y_C with the experimental minimum bias rapidity distribution from Ref. [18]. The minimum bias curve was fitted in the form (2.14) with $\langle n(s)\rangle$ from Ref. [15] and $dn/dy|_{y=0}$ from Ref. [19].

With rising y_C and $p_{\perp C}$ a clear asymmetry in the background distribution appears. The maximum of the distribution is shifted relative to $y = 0$ in opposite direction with respect to the trigger rapidity. In the cms rapidity hemisphere of the trigger position the

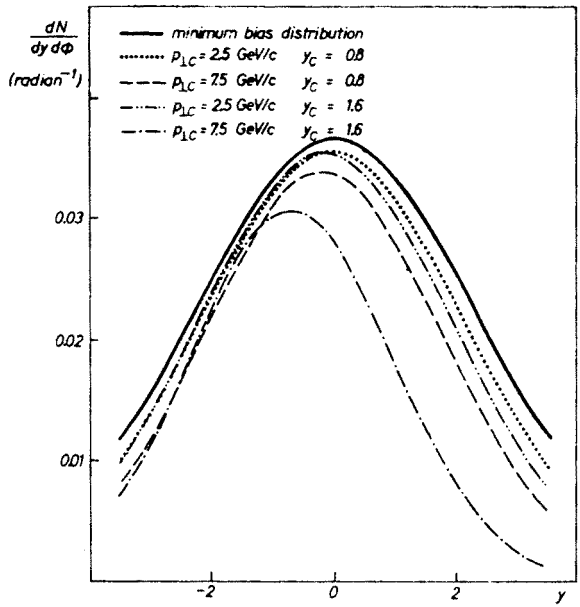

Fig. 5. Comparison of the associated background rapidity distribution for $y_G = 0.8$, 1.6 and $p_{\perp C} = 2.5$ GeV/c, 7.5 GeV/c with a parametrized minimum bias rapidity distribution [18]

particle yield arising from the low $p_\perp$ component decreases considerably. This decrease rises with $p_{\perp C}$ and y_C.

We conclude: The model contains no correlations except kinematical ones between the large $p_\perp$ and low $p_\perp$ component. However in this model the effects of overal energy--momentum conservation are important already at available presented trigger transverse momenta. With increasing $p_{\perp C}$ the associated total multiplicity first rises, reaches a maximum and finally decreases towards the kinematical limit. The initial rise is absent for same side multiplicities, it is more pronounced on the opposite side one. In order to understand the right magnitude for associated same and opposite side multiplicities we have to take into account the parton transverse momenta. We find the low $p_\perp$ component in the presence of large $p_\perp$ triggers to differ considerably from the minimum bias distribution. This effect rises with increasing trigger $p_{\perp C}$ and cms rapidities.

The author is grateful to Professor J. Ranft for suggesting the problem and constant help.

REFERENCES

[1] P. Darriulat, Rapporteur's talk, *Proc. of the 18th Int. Conf. on High Energy Physics*, Tbilisi 1976.
[2] P. V. Landshoff, Review talk, *Proc. of the 7th Int. Colloq. on Multiparticle Reactions*, Tutzing/Munich 1976.

[3] M. Della Negra et al., *Nucl. Phys.* **B127**, 1 (1977).
[4] S. J. Brodsky, J. F. Gunion, *Proc. of the 7th Int. Colloq. on Multiparticle Reactions*, Tutzing/Munich 1976.
[5] R. P. Feynman, R. D. Field, G. C. Fox, *Nucl. Phys.* **B128**, 1 (1977).
[6] J. Abad, A. Cruz, J. L. Alonso, *Nucl. Phys.* **B115**, 533 (1976).
[7] J. Kripfganz, J. Ranft, *Nucl. Phys.* **B124**, 351 (1977).
[8] E.-M. Ilgenfritz et al., *Acta Phys. Pol.* **B9**, 15 (1978); A. Schiller et al., *Acta Phys. Pol.* **B9**, 31 (1978).
[9] R. D. Field, R. P. Feynman, *Phys. Rev.* **D15**, 2590 (1977).
[10] J. Kripfganz, unpublished, see Ref. [8].
[11] J. D. Bjorken, *Phys. Rev.* **D8**, 4098 (1973); S. D. Ellis, M. B. Kislinger, *Phys. Rev.* **D10**, 891 (1974).
[12] J. Ranft, G. Ranft, *Nucl. Phys.* **B110**, 493 (1976).
[13] J. Ranft, G. Ranft, *Acta Phys. Pol.* **B8**, 179 (1977); *Acta Phys. Pol.* **B8**, 275 (1977).
[14] R. Kephart et al., *Phys. Rev.* **D14**, 2909 (1976).
[15] Thome et al., CERN preprint 1977.
[16] J. Ranft, G. Ranft, Karl-Marx-Universität preprint KMU-HEP-77-04.
[17] B. L. Combridge, *Phys. Rev.* **D12**, 2893 (1975); G. C. Fox, Caltech preprint 1976 CALT-68-573.
[18] M. Della Negra et al., CERN preprint, CERN/EP/PHYS 76-43.
[19] V. Blobel et al., *Nucl. Phys.* **B69**, 454 (1974).